SDSS'Rio 2010 STABILITY AND DUCTILITY OF STEEL STRUCTURES
E. Batista, P. Vellasco, L. de Lima (Eds.)
Rio de Janeiro, Brazil, September 8 - 10, 2010

STABILITY AND DUCTILITY OF CASTELLATED COMPOSITE BEAMS SUBJECTED TO HOGGING BENDING

Marian A. Gizejowski* and Wael A. Salah Khalil**

* Department of Building Structures, Warsaw University of Technology, Warsaw, Poland
e-mail: M.Gizejowski@il.pw.edu.pl

** Department of Civil Engineering, Al-Azhar University, Cairo, Egypt
e-mail: waelcivil@hotmail.com

Keywords: Castellated Composite Beam, Hogging Bending, Distortional Buckling, Ultimate Strength.

Abstract. *This paper presents investigations on distortional stability and ductility behavior of steel-concrete composite beams subjected to hogging bending. These investigations advance the current knowledge in the field of perforated continuous or semi-continuous composite beams with regard to their ultimate strength. In total, twelve composite beam specimens were tested under hogging bending conditions that simulate the behavior multi-span beams over their internal supports. Two sets of specimens were tested. Six long-span beam specimens represented cases where flexure controlled the behavior of composite beams, and the remaining six specimens were short-span for which the effect of shear could not have been neglected. Three groups of two identical beams with square, hexagonal and circular openings were tested in each set. Numerical modeling and prediction formula for the ultimate strength are proposed and verified with use of experimental results obtained by the authors.*

1 INTRODUCTION

Steel-concrete composite beams in continuous or semi-continuous structural systems are subjected to both sagging and hogging bending. Research on the stability behavior and ductility performance of plain webbed composite beams have been carried out extensively both experimentally and numerically for different beam static schemes, length-to-depth ratios, ratios of the concrete slab section area to the structural steel cross section area, reinforcement ratios, among others. General design rules for the resistance check of composite beams under sagging and hogging moments have been developed and introduced to current structural codes, e.g. to Eurocode 4, as a result of these extensive investigations. The restrained distortional buckling (RDB) of statically indeterminate plain webbed composite beams was dealt with by the authors in [1]. A direct strength method analytical formulation has been developed for the RDB assessment of composite multi-span beams as an alternative approach to those given in current codes of practice. The prediction equation has the form:

$$\frac{\Lambda_{b,dsm}}{\Lambda_{pl}} = \left(\alpha_1 - \alpha_2 \frac{1}{\bar{\lambda}}\right)\frac{1}{\bar{\lambda}}, \qquad \bar{\lambda} = \sqrt{\frac{\Lambda_{pl}}{\Lambda_{cr}}} \tag{1}$$

In equation (1) the following notation is used: Λ_{cr} - elastic distortional buckling load factor, Λ_{pl} - in-plane limit load factor, $\Lambda_{b,dsm}$ - RDB strength factor from *dsm* approach, α_1 and α_2 - constants.

Research on the behavior of castellated composite beams has not been carried out so extensively. Five castellated composite beams of different span lengths were tested up to failure at the Structural Engineering Laboratory of McGill University by Megharief [2]. The aim of his research project was to

observe the out-of-plane stability of posts separating the openings and the beam modes of failure under sagging bending, and then to model their behavior numerically with use of the finite element (FE) technique. A comprehensive experimental investigation of steel and concrete composite girders behavior under hogging moments was recently reported by He et al. [3]. Less attention, if any, has been paid to buckling phenomena of castellated composite beams under hogging bending, especially with reference to the length of hogging moment spread and different shape of openings. This paper presents the results of research project carried out at the Warsaw University of Technology (WUT) and concerned with the experimental investigations, numerical modeling and development of prediction equation for the buckling strength of continuous castellated composite beams. Developed FE modeling technique captures globally the effect of geometric and material imperfections. Validation of this modeling technique is presented by the comparison of the FE load-displacement characteristics with their experimental counterparts. Finally, it is proved that the prediction equation developed in [1] for the buckling strength of plain webbed composite beams may also be used for the prediction of RDB strength of castellated composite beams.

2 EXPERIMENTAL INVESTIGATIONS

Two sets of composite beam specimens were tested in the WUT laboratory, namely the set made of steel grade S355 and the set made of steel grade S420. The specimens of each set were divided into two subsets according to their span length, namely short-span specimens of 2116 mm beam length and long-span specimens of 4232 mm beam length. Each specimen consisted of two equal length spans, one overhanging with perforated web, and the other being plain webbed and supported at both ends. The overhanging span was loaded in such a way that both spans were under hogging bending (see figure 1).

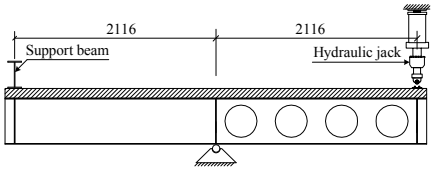

a) General layout and boundary conditions of long-span tested specimens

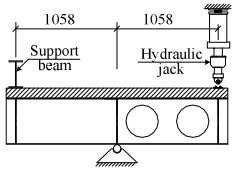

b) General layout and boundary conditions of short-span tested specimens

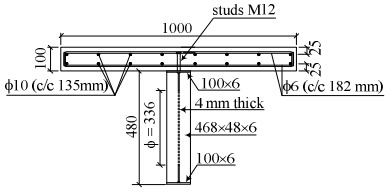

c) Typical beam cross-section at the centre of web opening

Figure 1: General layout of tested specimens.

Three different shapes of web openings were considered, namely rectangular, hexagonal and circular of equal opening area and the same c/c distance. The perforated span for long-span beam specimens consisted of four openings while two openings were designed for the web of short-span beam specimens. The list of the tested composite beams is shown in table 1.

Table 1: Description of tested composite beams

Specimen	Span length (mm)	Shape of openings	Number of openings	Steel grade
C4S355	2116	Circular	4	S355
C4S420	2116	Circular	4	S420
H4S355	2116	Hexagonal	4	S355
H4S420	2116	Hexagonal	4	S420
R4S355	2116	Rectangular	4	S355
R4S420	2116	Rectangular	4	S420
C2S355	1058	Circular	2	S355
C2S420	1058	Circular	2	S420
H2S355	1058	Hexagonal	2	S355
H2S420	1058	Hexagonal	2	S420
R2S355	1058	Rectangular	2	S355
R2S420	1058	Rectangular	2	S420

2.1 Test rig setup and loading program

The general layout of the test rig setup is shown in figure 2. Roller hinged support was inserted in the mid-length of the bottom flange of both long-span and short-span specimens where lateral movement was not allowed. At the left end of each tested specimen a steel tie frame fixed to the lab floor was provided in order to restrict lateral and upward vertical displacements. The right end was free to move vertically. The lateral displacement of the specimen at the right end was prohibited by means of two I-section bracing columns fixed to the lab floor, as illustrated in figure 2.

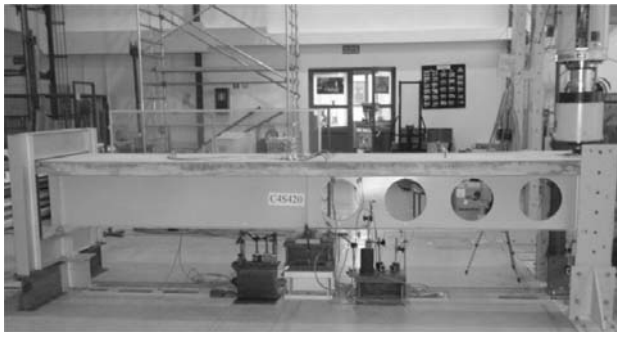

Figure 2: General arrangement of test rig.

The loading program was displacement controlled. The vertical displacement was applied gradually to the specimen starting from the elastic region of beam deformations, through the limit point attainment on the equilibrium path and up to excessive beam deformations in the post-limit range. At each of displacement increments, readings from strain gauges, displacement transducers and inclinometers were recorded in order to examine specimen in-plane and out-of-plane displacements and rotations. The surface of concrete slab was carefully inspected for the crack development and propagation. Testing was terminated in the post-limit range when the specimen displacements and rotations became large with reference to

normal service conditions, and the slab exhibited values of considerably wide concrete cracks. The displacement controlled by the actuator was then incrementally decreased and its residual value at the point of zero reactive force response of tested specimens was recorded.

2.2 Failure modes and ductility behavior

The failure mode of all the tested web perforated composite beams was associated with distortional instability. Various RDB modes were detected in which lateral-distortional mode with a small contribution of torsional deformations was a dominating mode for long-span beams with circular and hexagonal web openings. The torsional-distortional mode with a relatively small contribution of lateral deformations governed the behavior of long-span specimens with rectangular web openings and all the short-span specimens, regardless the opening shape type. The castellation process using square web openings created web posts with the lowest out-of-plane stiffness and with the highest stress concentration at the opening sharp corners. These factors were responsible for the torsional-distortional instability mode to occur before any significant lateral displacements seen to be developed.

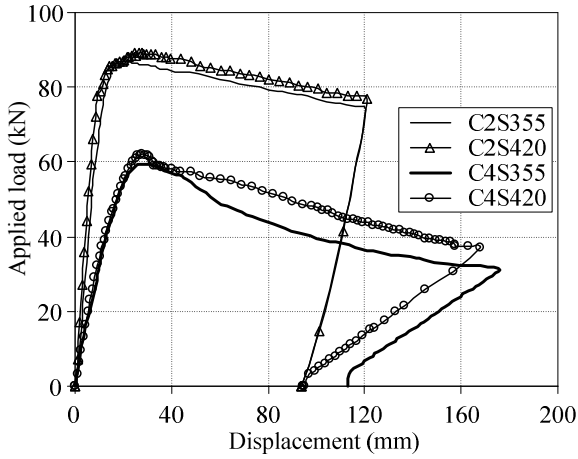

Figure 3: Load-displacement response of composite beams with web circular openings.

Figure 3 presents typical curves of the specimen reactive force vs applied vertical displacement for beams with web circular openings. The long-span beams show lesser initial stiffness and the lower ultimate load if compared with the corresponding values of the short-span specimens. This is quite understandable since the longer overhanging span means longer hogging moment length, and hence earlier triggering of the distortional buckling of unrestrained bottom flange of the structural steel profile. Moreover, the ultimate load of the long-span specimens does not depend significantly on the grade of structural steel the profile is made of. The same observation is valid for short-span specimens. This is attributed to early distortional instability that occurs before the commencement of yielding zones in the beam bottom flange. Since the beam buckling starts in the quasi-elastic region, the limit load is achieved with a limited yielding of the beam sections and substantial plastic deformations may only be developed in the post-limit range. Hence, the difference in the equilibrium path with regard to steel grade becomes noticeable in figure 3 for the post-limit beam responses. Beams made of the higher steel grade loose their stiffness less rapidly and approximately in a similar way with regard to different span lengths. Contrarily, beams with the lower steel grade exhibit different sensitivity to the stiffness decrease in the post-limit range. Short-span beams behave in this region in more a less the same way as those made of the higher steel grade. The stiffness of long-span beams made of the lower steel grade decreases more rapidly than

their higher steel grade counterparts. This is indicative to a better ductility performance of beams made of higher steel grade.

Summarizing the effect of web opening shape on the beam instability behavior, one can conclude that beams with hexagonal web openings represent very close behavior to those with circular openings. Beams with circular and hexagonal web openings are less exposed to the local effect of residual stress concentration at opening surroundings. Beams with hexagonal openings may however be in some cases more vulnerable to web plate fracture since their openings have the circumference line that is not curvilinear. Experiments concerned with the response of short-span beams with hexagonal web openings have shown that reaching the limit point on the equilibrium path is associated with the web plate fracture initiated from the corners of the opening being at the closest distance from the beam end. Reduction in the ductility performance is even more severe for beams with rectangular openings since the ultimate load of these beams, regardless of the beam span length, was always associated with the web plate fracture. Beams with rectangular web openings exhibited in tests lesser initial stiffness from their counterparts with circular and hexagonal web openings, and also the lower ultimate strength.

The effect of span length is affecting not only the mode of failure, ultimate strength and the post-limit response but also the development and pattern of concrete cracks of the composite beam slab. Crack patterns perpendicular to the beam axis formed in an early stage of loading in the slab of tested long-span beams and propagated in the post-limit state, reaching large values at the end of tests. This was indicative to the flexural response of composite beams. Patterns with diagonal cracks were observed for short-span beams indicating the contribution of concrete to the load transfer by shear.

3 NUMERICAL INVESTIGATIONS

The FE computer code ABAQUS is used to simulate the behavior of tested composite beams. Structural steel is modeled with use of thin shell finite elements S4R5 while the concrete slab with use of thick shell finite elements S4R. Options available in the ABAQUS library are used for constitutive models of structural steel, shear connectors and reinforced concrete. Huber-von-Mises yield criterion is used for steel while Smeared Cracks failure criterion is used for concrete in tension. Rebar Layer option allows to model the effect of reinforcement in the concrete slab. Mechanical properties of steel and concrete are derived from material tests. Since concrete tests did not provide data for all the parameters of constitutive models to be precisely evaluated, some of model parameters are calibrated on the basis of successive fitting of numerical model to the global behavior of tested specimens. A bilinear stress-strain diagram is used for steel behavior of shear connectors and reinforcement. Imperfections of structural steel are taken into consideration. Residual stresses of welded castellated steel profiles are globally represented by an equivalent curvilinear stress-strain characteristic accounted for stress hardening and gradual development of yielding (for details of this formulation see [4]). Patterns of geometric imperfections are conventionally modeled using a linear combination of eigenmodes with the maximum coordinate evaluated on the basis of survey conducted prior to testing for the geometry of initially distorted beam profiles. Eigenmodes are evaluated from elastic stability analysis option in ABAQUS and automatically incorporated to the imperfect model of beams for consideration in geometrically nonlinear analysis accounted for elastic-plastic properties of steel and inelastic behavior of concrete in compression and tension. Structural steel section dimensions are taken at the lower values obtained from measurements conducted for all the specimens just after the delivery from the manufacturer and before their final arrangement as the composite specimens for testing.

The behavior of tested specimens is examined by including the load-displacement analysis of Riks type and using an imperfect model of tested beams with imperfections modeled as described above. In the first analysis step, imperfect beams are subjected to a pressure load applied to the top flange that simulates the existence of an initial stress state due to the self-weight of the concrete slab. Then, the second load step commences by applying the vertical displacement at the point of actuator placement to simulate tests conducted in the laboratory in order to trace the specimen behavior under applied load.

Analysis is terminated at a point that over-passes the maximum vertical displacement recorded in tests, and the unloading stage recorded in testing is not simulated in numerical analysis.

3.1 Beam load-displacement characteristics and restrained distortional buckling strength

Load-displacement curves obtained experimentally are compared with numerical characteristic for all the tested specimens. Figures 4 and 5 illustrate the results for beams with circular web openings of long-span and short-span specimens, respectively. Load-displacement characteristics obtained by FE analysis can reproduce with high degree of accuracy the actual performance of tested composite beams with circular web openings with respect to the initial stiffness, RDB strength and the post-limit behavior. The prediction for other beam load-displacement curves is a bit less accurate, especially for those that experience the web plate fracture. Fracture phenomenon can not be captured in numerical analysis. Because the web plate fracture was detected in tests at the load level corresponding to the limit point, it affected significantly the post-limit branch of the equilibrium path. FE simulations over-predict experimental results. After reaching the ultimate strength, the experimental load-displacement curves of fractured specimens start to sharply degrade while FE curves exhibit much slower degradation.

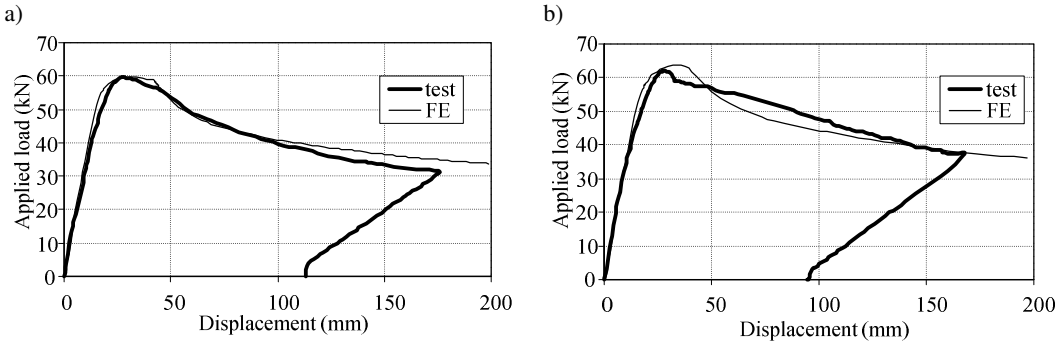

Figure 4: Load-displacement characteristics - long-span beams with circular openings; a) S355, b) S420.

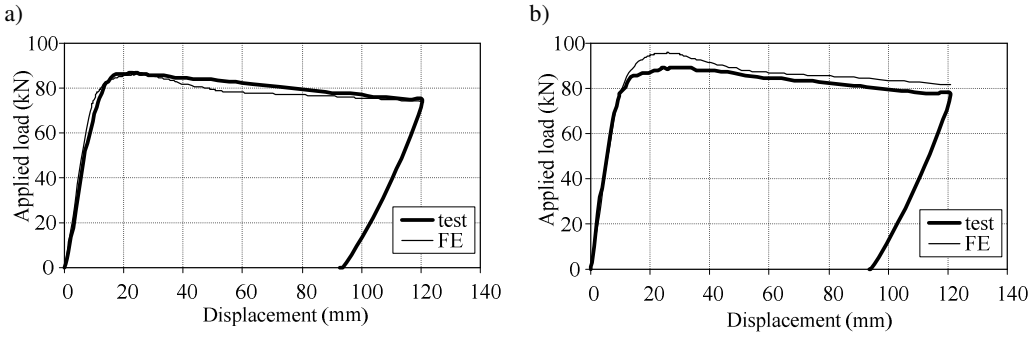

Figure 5: Load-displacement characteristics - short-span beams with circular openings; a) S355, b) S420.

Table 2 summarizes all the results of tested beams with regard to the ultimate load obtained experimentally and numerically. Differences between the experimental RDB loads and their numerical counterparts are up to 7% with exception of R2S420 for which the web plate fracture occurred much earlier than for the other beams with rectangular openings. For the beam R2S420 the difference between the experimental and numerical ultimate loads appears to be at the maximum value of 14%.

Table 2: Comparison of experimental and numerical values of beam ultimate load

Specimen	Experimental ultimate load (kN)	Numerical ultimate load (kN)
C4S355	59,6	59,6
C4S420	62,3	63,7
H4S355	62,0	59,3
H4S420	62,5	63,5
R4S355	50,2	51,7
R4S420	53,1	57,1
C2S355	86,7	86,2
C2S420	89,4	95,7
H2S355	87,6	85,9
H2S420	88,9	95,3
R2S355	73,4	78,3
R2S420	74,9	85,7

3.2 Beam deformations

The accuracy of numerical modeling technique developed may also be checked comparing deformed profiles of distorted beam sections obtained for the post-limit range of deformations. Deformed profiles of tested beams recorded in the laboratory are compared with the corresponding profiles obtained from numerical analysis. Figures 6 and 7 illustrate the comparison of deformed profiles for the same value of vertical displacement, for the cellular long-span and short-span beams, respectively. Deformed profiles obtained experimentally and numerically are very close to each other. The similar results are obtained for other tested specimens.

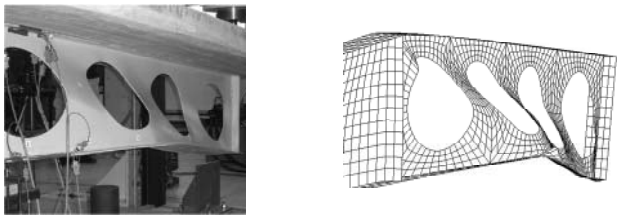

Figure 6: Experimentally and numerically obtained deformed profiles of specimen C4S420.

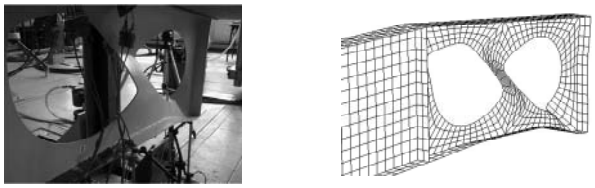

Figure 7: Experimentally and numerically obtained deformed profiles of specimen C2S420.

Deformed profiles obtained numerically for web perforated composite beams confirm that composite beams of slender sections fail under hogging bending in the distortional buckling mode before achieving the beam in-plane Vierendeel mechanism load. Advanced FE Riks analysis based on imperfect model of real beams proves to be highly accurate when modeling the load-displacement behavior of both long-span and short-span beams, and their RDB strength. The results obtained with use of such an analysis may therefore be used for the wider research project of getting a representative number of point corresponding

to the RDB ultimate strength of continuous composite beams of different cross-section types, slab section areas and material properties. These points may next be used for calibration of simplified methods recommended for the practical assessment of composite beam buckling strength.

4 DIRECT STRENGTH METHOD PREDICTION EQUATION

The buckling strength equation (1) based on the direct strength method (referred to *dsm* equation hereafter) was proposed in [1] for the assessment of buckling strength of continuous plain webbed composite beams. In the following, the hypothesis is verified whether this equation is of a general nature and can be used also for the prediction of RDB strength of castellated composite beams, or not. In order to validate equation (1) for castellated composite beams, authors own experimental ultimate loads are used herein, instead of numerical results. Validation is given in figure 8. Experimental values $\Lambda_{b,\exp}/\Lambda_{pl}$ are calculated and marked in figure 8 by points representing test results for castellated composite beams with circular, hexagonal and rectangular openings. Test results are compared with the analytical predictions from equation (1) represented in figure 8 by the curve. From this validation exercise one can conclude that *dsm* equation developed in [1] can be successfully used also for the safe prediction of distortional buckling strength of castellated composite beams under hogging bending.

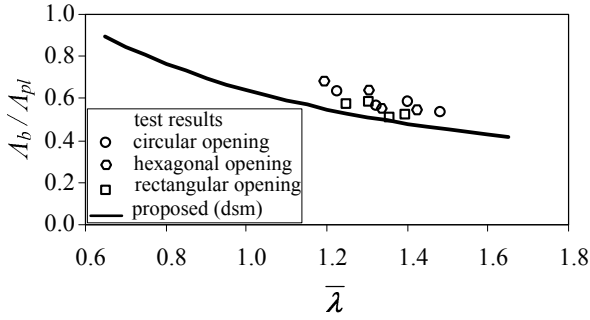

Figure 8: Validation of direct strength method applicability to web perforated composite beams.

5 CONCLUSIONS

Results of experimental investigations, advanced numerical analysis and analytical RDB strength formulation of perforated web composite beams under hogging bending are presented. Ultimate loads are predicted and compared, together with the identification of distortional buckling modes and ductility performance. Results obtained advance current knowledge on the stability and ductility behavior of castellated composite beams made of slender structural steel sections.

REFERENCES

[1] Salah, W. and Gizejowski M.A., "Restrained distortional buckling of composite beams – FE modelling of the behaviour of steel-concrete beams in the hogging moment region", *Proc. of EUROSTEEL2008 5th European Conference on Steel and Composite Structures*, R. Ofner et al. (eds.), ECCS Publication, Brussels, 1629-1634, 2008

[2] Megharief, P.S., *Behavior of Composite Castellated Beams*, McGill University, Montreal, 1997.

[3] He, J., Liu, Y., Chen A. and Yoda, T. "Experimental sudy on inelastic mechanical behaviour of composite girders under hogging moment". *Journal of Constructional Steel Research*, (in press).

[4] Gizejowski, M.A., Salah, W., Barcewicz, W. "Finite element modeling of the behaviour of steel end-plate beam-to-column joints". *Archives of Civil Engineering*, **LIV**(4), 693-733, 2008.